



## Study of through thickness effects by means of the stress intensity factor

A. Gonzalez-Herrera<sup>1</sup>, J. Garcia-Manrique<sup>2</sup>, D. Camas<sup>3</sup>, P. Lopez-Crespo<sup>4</sup>

*Departamento de Ingeniería Civil, de Materiales y Fabricación, Universidad de Málaga, Málaga (Spain)*

*<sup>1</sup>agb@uma.es; <sup>2</sup>josegmo@uma.es; <sup>3</sup>dcp@uma.es; <sup>4</sup>plopezcrespo@uma.es;*

**ABSTRACT.** The study of crack tip fields is often conducted assuming a homogeneous behaviour through the thickness. Depending on the specimen thickness, a state of plane stress or plane strain is normally presumed. However, recent studies have shown a more complex behaviour along the thickness. On the one hand, plasticity-induced crack closure effects affect mainly to a small region close to the specimen surface. On the other hand, the plastic zone evolution along the thickness is not as simple as the classic dog-bone shape normally described in Fracture Mechanics textbooks. Unlike what is normally expected, the size of the plastic zone decreases in a very small region close to the surface, as we move from the interior of the specimen to the specimen surface. These two effects can be detected if the mesh used in the finite element model is sufficiently fine. Both effects are probably related to an uneven distribution of the load along the thickness. One of the consequences of these effects on the fatigue crack growth is the curvature of the crack front. Nevertheless, this curvature can be explained by two mechanisms. The first one is related to the crack closure effect near the surface, it would imply a smaller effective  $\Delta K$  close to the surface, and therefore a slower crack growth rate. The second one (plastic zone size decrease close to surface) is probably due to  $\Delta K$  being smaller near the surface than in the interior. The current work attempts to evaluate numerically both effects in order to separate their individual influence and their magnitude. This is done by evaluating the  $K$  distribution along the thickness at different planes on an Al 2024-T35 compact tension specimen. The plastic wake effect is removed from the model in order to distinguish between both effects.

**KEYWORDS.** Finite element analysis; Crack growth; Plastic wake; Fatigue crack closure; Stress intensity factor (SIF).

### INTRODUCTION

The study of crack tip fields is often conducted assuming a relatively simple behaviour through the thickness. Depending on the specimen thickness, a state of plane stress or plane strain is normally presumed. In the more general case, a small linear transition is normally presumed [1]. However, recent studies have shown a more complex behaviour along the thickness. Fig. 1 shows the crack displacement field obtained by means of finite element (FE) calculations in an 3D crack. These images correspond to the simulation of the fatigue crack growth in a CT specimen. Straight crack front is considered. Plastic crack wake has been developed by cycle by cycle crack advance. The methodology applied can be consulted in [2]. The load case correspond to  $R = 0.3$ ,  $b = 3$  mm.  $K_{\max} = 25$  MPa·m<sup>1/2</sup>. Vertical displacement of the crack flanks near the crack are shown at minimum load,  $K_{\min}$ , (Figure 1a) and maximum load,  $K_{\max}$  (Fig. 1b). The mid plane of the specimen is that of the top right corner, and the free surface of the specimen is on the bottom left corner in Figure 1. Different qualitative issues can be observed. It can be seen that plasticity-induced crack closure affects mainly to a small region close to the specimen surface. Only one line of nodes is in contact in the interior



zone while all the area where the plastic wake has been simulated is in contact at minimum load in a region very close to the exterior. In addition, if we observe the crack opening displacement (COD) at  $K_{\max}$  (Fig. 1b) it is higher at the interior than the exterior.

Considering the evolution of the plastic zone along the thickness in Fig. 2, it can be seen that it is not as simple as the classic dog-bone shape normally described in Fracture Mechanics textbooks [1]. A number of different cases with varying values of  $R$ ,  $K_{\max}$  and  $b$  were simulated. The same qualitative behaviour was observed for all cases, thus Figure 2 is representative of the general behaviour. Unlike what is normally expected, the size of the plastic zone decreases in a very small region close to the surface, as we move from the interior of the specimen to the specimen surface. These effects can only be detected if the mesh used in the FE model is sufficiently fine. With current computational power, this limits the number of simulations to be made.

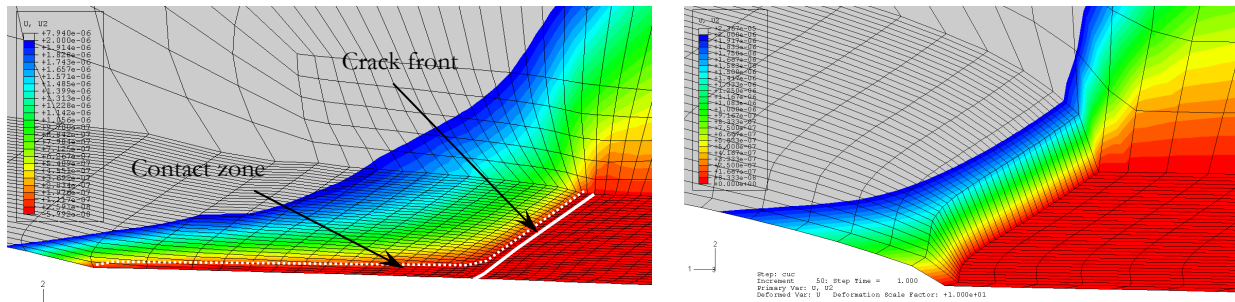


Figure 1: Vertical displacement of the crack plane,  $u_y$  (m), at (a) minimum load,  $K_{\min}$  and (b) maximum load,  $K_{\max}$ , with  $R = 0.3$ ,  $b = 3$  mm.  $K_{\max} = 25 \text{ MPa}\cdot\text{m}^{1/2}$ . Fatigue crack closure simulation was conducted assuming straight crack front.

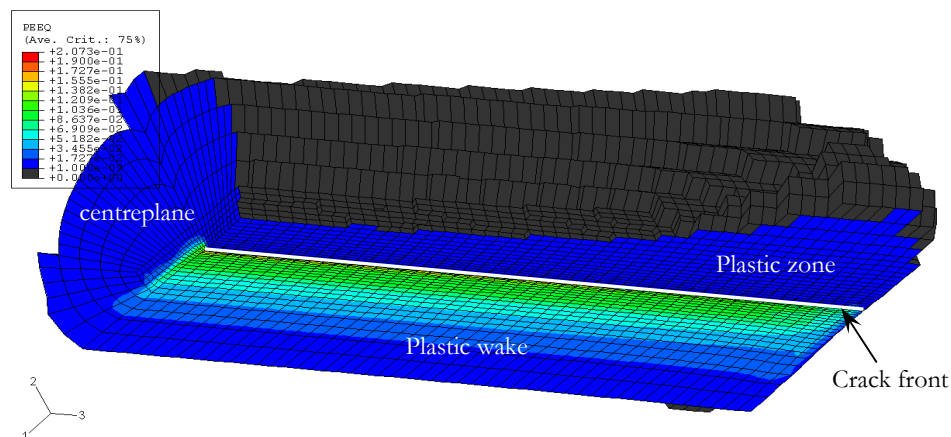


Figure 2: Plastic zone and plastic wake. Fatigue crack closure simulation with straight crack tip.  $R = 0.3$ ,  $b = 6$  mm.  $K_{\max} = 20 \text{ MPa}\cdot\text{m}^{1/2}$ . The mid plane across the thickness is located to the left of the figure, and the free surface to the right.

The curvature of the crack is one of the experimental evidences that can be explained as a direct consequence of these effects. When a crack grows on a fatigue process the crack front changes adopting a curved shape. The crack grows faster at the interior than at the exterior. This curvature can be explained by two mechanisms which are difficult to evaluate separately. The first one is related to the crack closure effect near the surface. As the load is applied, opening is first at the interior, and later at the exterior zone. This implies a smaller effective  $\Delta K$  close to the surface, and therefore a slower crack growth rate. This effect is schematically depicted in Fig. 3a. This has been evaluated in 3D-FE model studies where plasticity induced crack closures has been included [2, 3]. The ratio  $\Delta K_{\text{eff ext}}/\Delta K_{\text{eff int}}$  was about 0.5, being affected by the value of  $R$ , the specimen thickness and load case. These calculations were made considering a straight crack tip. A fine mesh at the exterior was used.

The other mechanism to explain the fact that the crack grows faster in the interior than at the surface is related to the observance of plastic zone size along the thickness. As it is shown in Fig. 2, this decreases unexpectedly in a region close to the surface. In this case, this mechanism is not directly related to crack closure effect. It can be considered caused by

the elastic-plastic strain field resulting from the strong different constraint conditions at the interior and the exterior of the crack tip. As a consequence, a smaller  $K$  value is present near the surface (and then a  $\Delta K$  smaller, Fig. 3b) than in the interior causing a smaller plastic zone than the expected value with plane stress condition.

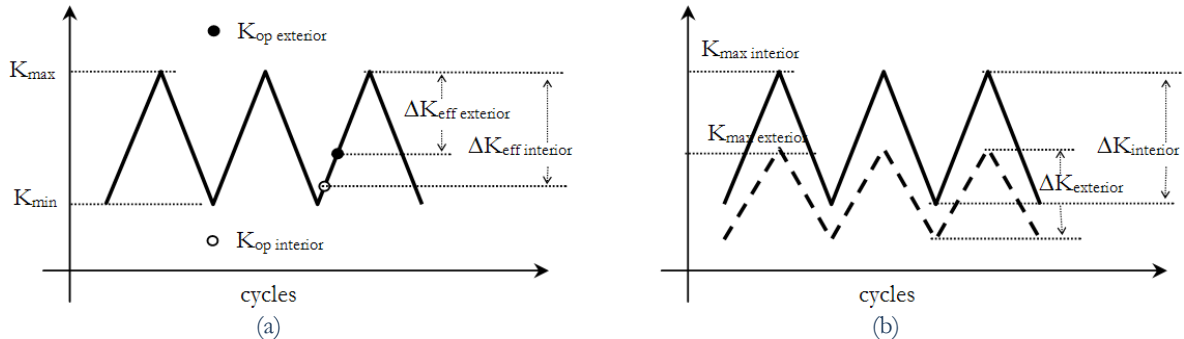


Figure 3: Differences in  $\Delta K_{\text{eff}}$  along the thickness due to (a) crack closure or (b) constraint conditions.

There exists probably interference between both effects. Branco et al. [4] developed an interesting work in order to evaluate how these effects could model the curvature of the crack front. They used FE calculations to obtain  $\Delta K_{\text{eff}}$  at different position along the thickness. They applied these values to evaluate the crack growth rate at this position. They found that a stable crack curvature was achieved independently from the starting shape. A limitation in the through-thickness meshing and the technique employed to evaluate  $K$  limited the extension of their conclusions.

The current work is a first step to evaluate numerically these effects but separately. In this case the plastic wake effect is removed from the model in order to distinguish between both effects.  $K$  distribution along the thickness at different planes is evaluated on a 3D-FE model of an Al 2024-T35 compact tension (CT) specimen.

## METHODOLOGY

Two key aspects are involved in the numerical modelling of this problem. The first one is the own FE model developing. The second one relates to the post-processing of the numerical results, in particular the technique to obtain the values of  $K$  and  $J$ -integral along the thickness.

### Finite Element Model

A specific methodology has been developed based on previous works focussed on the study of fatigue crack closure [2, 3, 5]. The methodology has been adapted to evaluate the evolution of  $K$  across the thickness. In order to remove the plastic wake effect, simulations were performed considering a single load applied to the specimen. No plasticity induced fatigue crack closure effect was included in the model.

The key aspect of this problem is that the plastic behaviour is concentrated in a small area surrounding the crack front. The main complexity in the numerical modelling is the drastic stress and strain gradient in the area surrounding the crack tip which must be properly captured with an appropriate mesh. This implies a very small element size at the crack front. The plastic zone size is the scale reference to relate to the minimum element size. In this work as in previous ones Dugdale's plastic zone size for plane strain has been used as a reference for determining the minimum element size of the mesh. In order not to penalize the computational cost, it is necessary to make a drastic transition from the crack tip region to the most remote ones. For this reason, the specimen has been divided in two different regions. In the first one, around the crack tip, a homogeneous and uniform undistorted mesh with hexahedral elements is made. The second region is meshed with tetrahedral elements which aid the transition. The minimum element size has been established following the recommendation from previous works [5] and the evolution of some parameters as the  $K$  and  $J$ -Integral results.

Between 20 and 40 divisions were considered in the mesh along the thickness direction in the crack tip region in all the cases shown in the present work. The number of divisions is defined as the ratio between the plastic zone size,  $r_{pD}$ , and the size of the smaller element next to the crack tip. Once the minimum element size is established, the number of the thickness divisions is decided. This is done in order to keep an acceptable element shape ratio and a correct solution in the surface zone. A shape ratio of 4 was adopted as limiting condition. However, in most of the elements the ratio did not



exceed 1.5. Outside the crack tip region, the number of through-thickness divisions was reduced to speed up the simulations. A good compromise between accuracy and computational cost was achieved by employing hexahedral prism shaped elements within the plastic zone and 8-node tetrahedral elements outside. In addition, the use of 8-node tetrahedral elements facilitated the transition between both zones.

The main feature of the models is the fine mesh along the thickness that is employed. This is a common feature with previous works [2, 3] and is a key issue, especially in order to interpret the results close to the exterior surface. In this study, common CT specimen geometry was modelled in 3D. Due to the symmetry and the loads applied, only a quarter of the specimen needs to be modelled. Different crack lengths were analysed, although only the results corresponding to  $a = 20$  mm are reported in this paper. In addition, different loads were applied, with the nominal SIF,  $K_{nom}$ , ranging from 10 to 30  $\text{MPa}\cdot\text{m}^{1/2}$ .

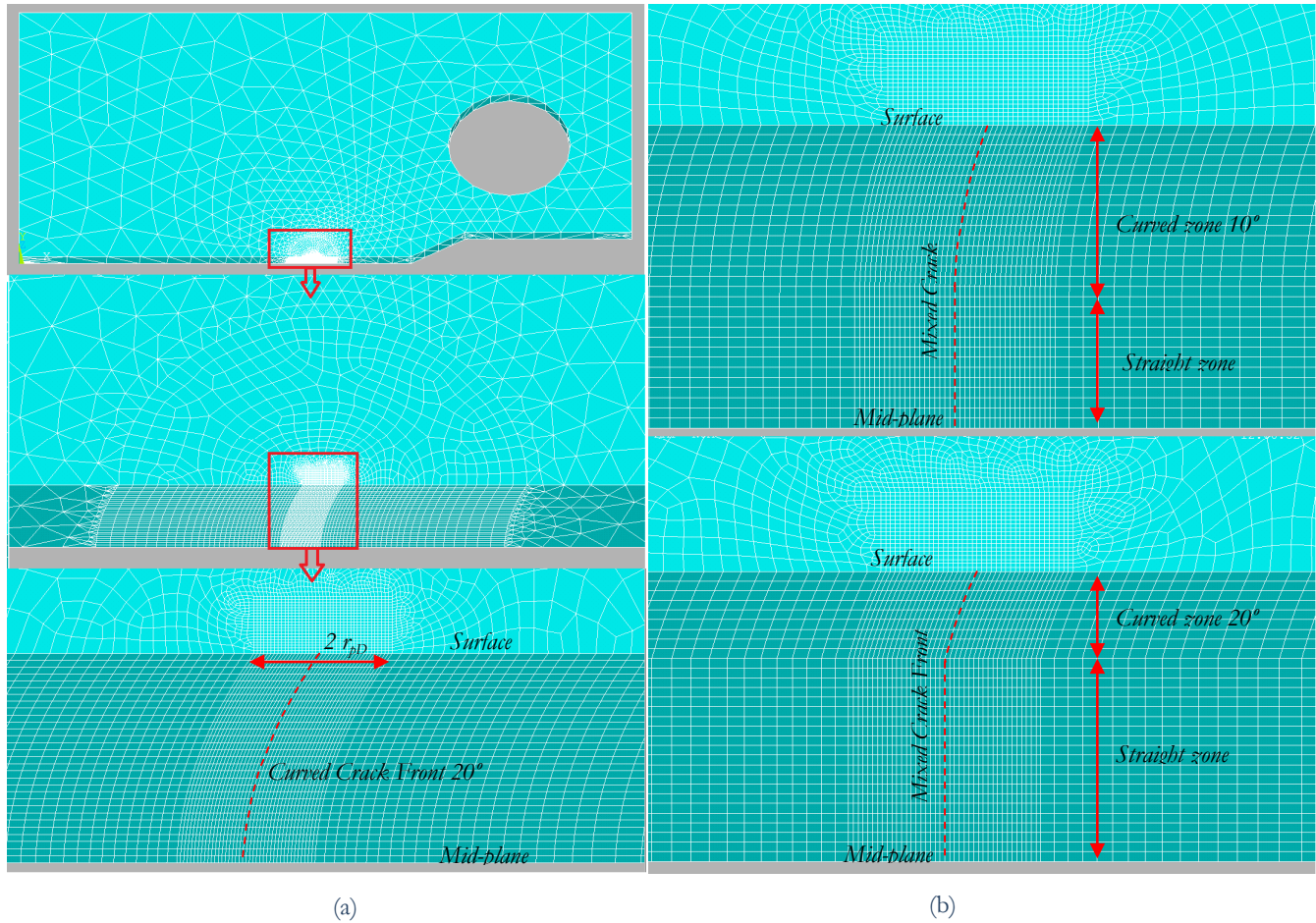


Figure 4: Finite Element Model: (a) Full model for a Curved Crack Front with 20° curvature angle. (b) Mesh around Crack Front in two mixed crack front, first one with 60% curved with 10° curvature angle and second with 40% curved with 20° curvature angle.

In this model (Fig. 4) the effect of the crack front curvature is also included. Different shapes of the crack front have been simulated and compared with straight crack hypothesis. In particular curved cracks with different curvature angles (10°-20°-30°) and mixed cracks curved only in the vicinity of the surface have been studied. In mixed shape cracks, the relative sizes between zones and the angle of curvature have been varied.

#### *K and J-integral numerical calculation*

It is a main issue in this kind of work to establish a consistent criterion to evaluate the SIF parameter along the thickness. It is affected by the theoretical approach to the problem as well as the FE model features as number and size of element or distance to the crack tip. We have evaluated the SIF related to  $K_{nom}$  that is usually employed in most fatigue and fracture studies. The  $K_{nom}$  for a compact tension CT specimen in mode-I is [6]:





$$K_{\text{nom}} = \frac{P}{b\sqrt{w}} \left( \frac{2 + \frac{a}{w}}{\left(1 - \frac{a}{w}\right)^{\frac{3}{2}}} \cdot \left( 0.886 + 4.64 \cdot \left(\frac{a}{w}\right) - 13.32 \cdot \left(\frac{a}{w}\right)^2 + 14.72 \cdot \left(\frac{a}{w}\right)^3 - 5.6 \cdot \left(\frac{a}{w}\right)^4 \right) \right) \quad (1)$$

where P is the load applied, b is the specimen thickness, w is the distance from the loading line to the specimen edge and a is the crack length.

Two methods have been considered to obtain K. The first method is based on the known relationship between the SIF and the perpendicular displacement to the crack face in linear elastic problem with a homogeneous isotropic material,  $K_{\text{cod}}$  [7]. This can be evaluated in each plane through the thickness employing the next formulation:

$$K_{\text{cod}} = \frac{\sqrt{2\pi} \cdot G}{1 + \kappa} A \quad \kappa = \begin{cases} = 3 - 4\nu & \text{Plane Stress} \\ = \frac{3\nu}{1 + \nu} & \text{Plain Strain} \end{cases} \quad \frac{|u_y|}{\sqrt{r}} = A + B \cdot r \quad (2)$$

where parameter A is obtained comparing displacement data ( $u_y$ ) from two nodes in the open crack, so the result is affected by the election of these nodes and the opening crack shape near the crack front.

The second method is based on the relation between the SIF and the contour integral calculation J-integral. An expression for J in its 2-D form is shown below. It assumes that the crack lies in the global Cartesian X-Y plane, with X parallel to the crack:

$$K_J = \begin{cases} \sqrt{J \frac{E}{(1 + \nu^2)}} & \text{Plain Strain} \\ \sqrt{J \cdot E} & \text{Plane Stress} \end{cases} \quad J = \int_r W dy - \int_r \left( t_x \frac{\partial u_x}{\partial x} + t_y \frac{\partial u_y}{\partial y} \right) ds \quad (3)$$

where W is the strain energy density (that is, strain energy per unit volume),  $t_x$  is the traction vector along x axis,  $t_y$  is the traction vector along y axis, u = displacement vector, s = distance along the path,  $\gamma$  = any path surrounding the crack tip. A routine was developed in ANSYS [8] to calculate the SIF in many perpendicular planes at multiple locations along the crack front to observe their evolution from midplane to surface. A great effort was dedicated to elucidate the influence of different path and distances from the crack for  $K_{\text{cod}}$  and  $K_J$  calculations, in order to correctly implement the simulation model. K was obtained in 2D at different distances with COD and J methods to compare the numerical mode with the theoretical one (Figure 5). Load level is represented as  $K_{\text{nom}}$ . It can be noticed from Fig. 5 that both of them reach the theoretical  $K_{\text{nom}}$ , both in plane strain and plane stress conditions (not included in Fig. 5). But a different behavior is observed. The value obtained with  $K_{\text{cod}}$  depends strongly on the selected node to calculate the value and becomes inaccurate for distances close to crack region. On the other hand, J-integral results converge quickly to the theoretical SIF for every path around the crack tip at any load level. Consequently, J-integral method was chosen to be the most suitable for evaluating the SIF in this case.

Once the numerical methodology is tested in 2D, it has been used in 3D models to calculate the SIF on planes parallel to the surface along the thickness with both methods. The results for the different loads levels, specimen thickness and crack shapes are shown in the following section.

## NUMERICAL RESULTS

**R**esults with different curvature shape (Fig. 6) versus straight crack front are shown in Figs. 7 and 8. Numerical data in curve and mixed crack front shapes are corrected with their exact crack length to K vs.  $K_{\text{nom}}$  comparison.

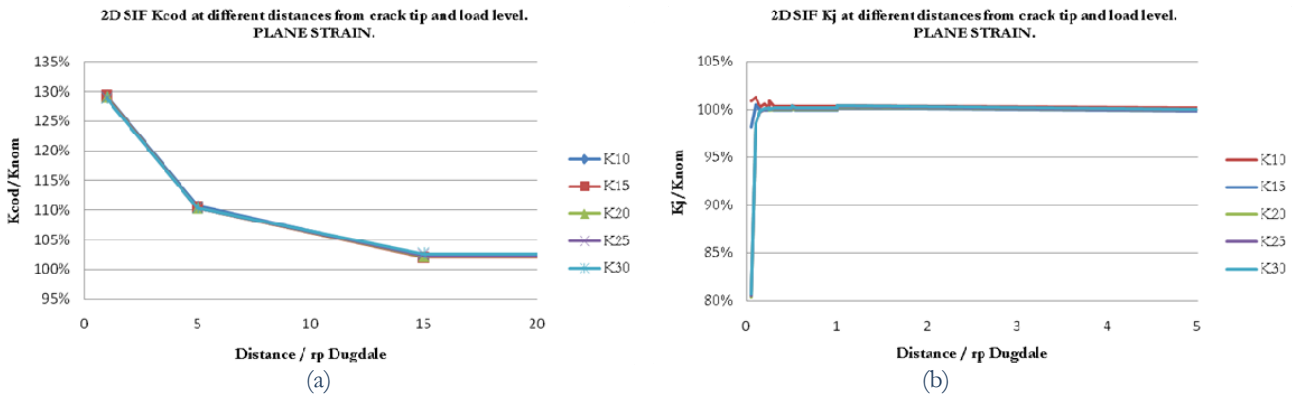


Figure 5: Differences in SIF results in 2D plain strain for multiples paths from the crack tip and different load levels a)  $K_{cod}$  method b) J-integral method. Each of the five plots is related to a different load, for example K20 means load for  $K_{nom}=20 \text{ MPa}\cdot\text{m}^{1/2}$ .

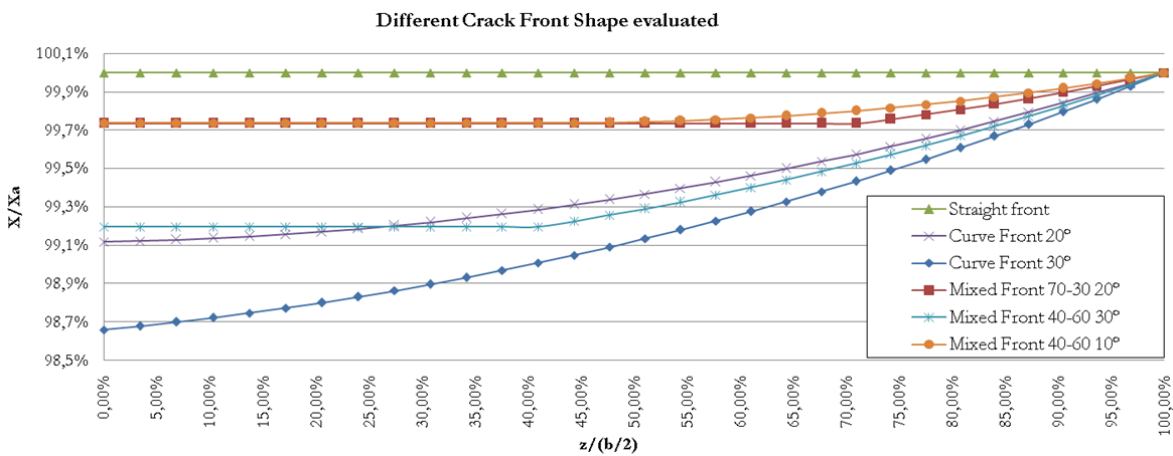


Figure 6: Different crack front shape evaluated (Straight, curved and mixed) in a  $b=3 \text{ mm}$  3D model.

If we observe  $K_{cod}$  results in Fig. 7a, a higher value than  $K_{nom}$  is obtained and it increases when we move to the exterior. This is not consistent with the plastic zone observed (Fig. 2) and is a consequence of the convergence difficulties of this method.  $K_{cod}$  results obtained stabilise at an interpolation distance above  $10r_{pD}$  (Figs. 5a and 7b) but not in the vicinity of the crack front. The problem is that at this distance ( $10r_{pD}$ ) the  $u_y$  distribution isolines are almost parallel so for a straight crack front,  $K_{cod}$  tends to the same value through thickness due to his dependence with  $u_y$ . Only evaluated close to the straight front ( $1r_{pD}$  path) the expected behaviour is obtained; nevertheless the value is distorted. This effect has more influence in a non straight crack front (Fig. 7a). The COD method use the same distances to measure  $u_y$  for each crack node. So with curved crack front,  $K_{cod}$  is proportional to the crack front shape leading to consider that the crack grows faster at the exterior. This is opposite to the observed behaviour.

As a consequence, the methodology based on COD formulation is not pertinent to evaluate the SIF to determinate parameter in the vicinity of the crack front. When Branco et al. [4] tried to obtain iso-K curvature shape, the problem was that with COD K based, all models tend to become in straight crack as this numerical effect balanced the crack closure effect at the exterior.

SIF J-integral based results are represented in Fig. 8. All data correspond with a path surrounding each crack node at a distance of  $r_{pD}$ . The integral along the thickness gives an average value of 103-105% of  $K_{nom}$  in all cases which is very approximate to the theoretical one. SIF distribution along the crack front is illustrated and presents a different behaviour depending on the crack shape considered. This means different crack growth rates along the crack front as is well known. It becomes an evident factor of the tunnelling effect.

With straight crack front, K is higher at the interior and decrease to the exterior with an abrupt transition at the surface. This is consistent with previous observation (Fig. 2, [2, 3]). If we evaluate the effect of the presence of the curvature (Fig. 8a) it can be seen that  $K_j$  decreases at the midplane when the curvature angle increases. This load seems to be transferred to the exterior. Nevertheless, at the most external region (above 95%), very similar values are obtained and the same abrupt transition is observed.



Curved front presents an excessive  $K_j$  reduction near midplane, it is opposite to empirical observation. This effect may be cancelled by using mixed shape curvatures. In these curved crack fronts, a straight front persists in midplane influence region and the curvature is reduced to the vicinity of the surface. Different configuration has been calculated (Fig. 8b). Higher curvatures displace  $K$  distribution from the midplane toward the surface.

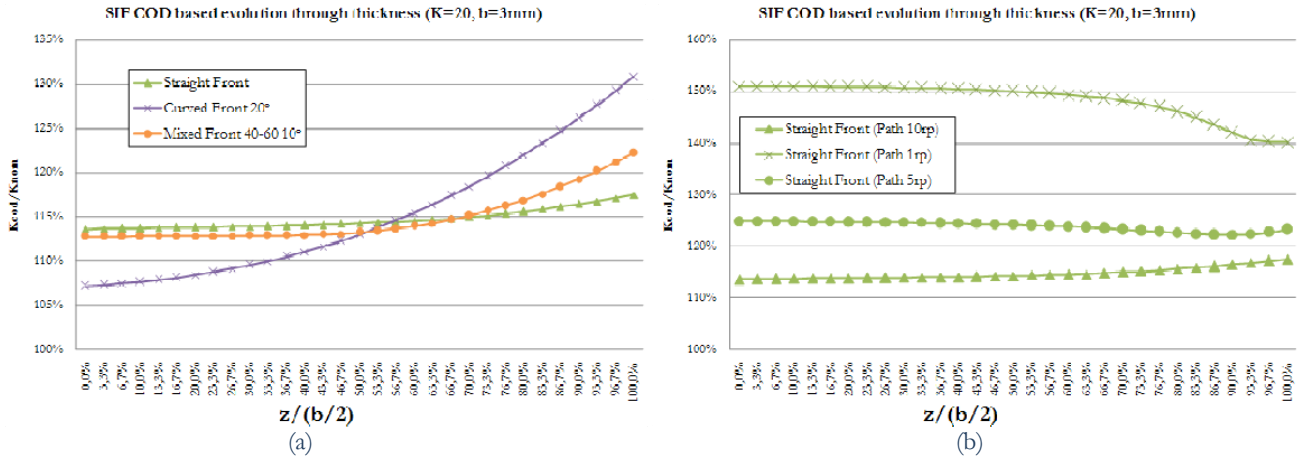


Figure 7: SIF COD based evolution through thickness ( $K=20 \text{ MPa}\cdot\text{m}^{1/2}$   $b=3\text{mm}$ ): (a) different shape crack front calculated at  $10r_{pD}$ . (b) results for Straight crack front, calculated at various distances (1-5-10 $r_{pD}$ )

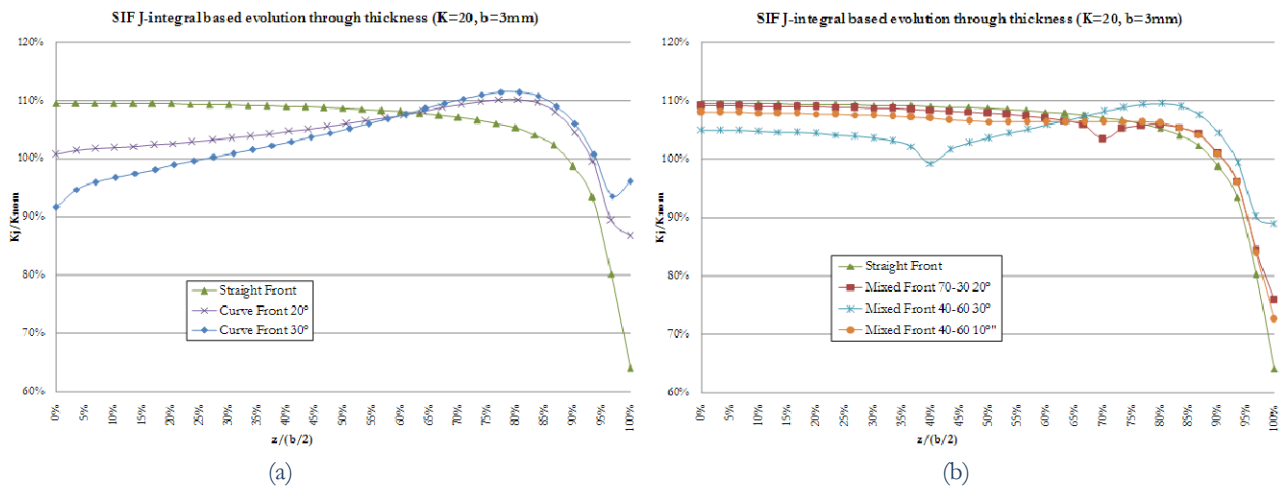


Figure 8: SIF J-integral based evolution through thickness for different crack front shape ( $K=20 \text{ MPa}\cdot\text{m}^{1/2}$   $b=3\text{mm}$ ): (a) Curved Fronts vs Straight Front. (b) Mixed Front vs Straight Front.

It could be expected that an intermediate position exists where iso- $K$  is reached. In the present model the limitation to evaluate this issue is that crack closure effect is not present. Nevertheless it can be seen that in the exterior, a smaller value of  $K_j$  is always present. That means that it will act as a limitation to the crack growth. According to this, the curvature would never tend to stabilize. This is not realistic. What these preliminary results show is that the interior curvature is not the only parameter to evaluate crack closure. At the exterior there exists a double singularity which must be studied carefully. The shape of the crack in this zone became a key aspect to understand how crack closure affects the whole crack growth.

## CONCLUSIONS EVALUATION

The current work demonstrates the existence of a number of through-thickness effects which are normally ignored in most of fatigue crack growth studies. An attempt is done to quantify their effect by means of 3D FE simulation. For this, an advanced FE methodology has been proposed. The methodology allowed us to infer the SIF



distribution along the specimen thickness in order to explore the importance of the thickness effects taking place.

Two different methods have been evaluated for obtaining numerically the SIF, namely one based on the COD and another one based on the J-integral. The J-integral based method proved to give better results in terms of accuracy and resolution in the region very close to the crack tip.

This tool was then used to study the evolution of the SIF along the thickness. It was observed that the SIF distribution along the thickness is very dependent on the crack curvature. It has been proved that not only the magnitude of the curvature is relevant; the shape of the curvature presents a huge influence.

This distribution will have influence in the growth rate of each node of the crack front and his dependence on shape implies a final invariant shape crack front for an invariant  $\Delta K$  and load level. In part, the shape of the curvature may lead to an ideally iso-K distribution along the thickness. However there is a small area at the exterior of the specimen where it is not possible. Additional research will be required to understand the 3D effects existing in the very vicinity of the surface, which is not properly captured by the numerical model.

It is critical to appreciate the gradient evolution of SIF near the surface with an adequate meshing through the thickness. Many authors do not usually consider this aspect in their numerical model and it might well be the reason to explain some of the non consistent results obtained in the literature.

## REFERENCES

- [1] H. L. Ewalds, R. J. H. Wanhill, *Fracture Mechanics*, Arnold, London (1984).
- [2] A. Gonzalez-Herrera, J. Zapatero, *Eng. Fract. Mech.*, 75 (2008) 4513.
- [3] A. Gonzalez-Herrera, J. Garcia-Manrique, A. Cordero, J. Zapatero, *Key Eng. Mater.*, 324-325 (1) (2006) 555.
- [4] R. Branco, D.M. Rodrigues, F.V. Antunes, *Fatigue Fract. Engng. Mater. Struct.*, 31 (2008) 209.
- [5] A. Gonzalez-Herrera, J. Zapatero, *Eng. Fract. Mech.*, 72 (2005) 337.
- [6] Y. Murakami, *Stress Intensity Factors Handbook*. Pergamon Press, Oxford (1987).
- [7] P. C. Paris, G. C. Sih, *ASTM, Philadelphia, STP 381* (1965) 30.
- [8] ANSYS, *User's manual*, 12.